Computers and Mathematics with Applications 61 (2011) 3639–3652

Contents lists available at ScienceDirect

Computers and Mathematics with Applications

journal homepage: www.elsevier.com/locate/camwa

A gas-kinetic BGK scheme for gas–water flow

Qibing Li *, Song Fu

Department of Engineering Mechanics, Tsinghua University, Beijing 100084, PR China

ARTICLE INFO

Keywords:
Gas-kinetic scheme
Gas–water two-phase flow
Mixture model

ABSTRACT

A new one-dimensional gas-kinetic BGK scheme for gas–water flow is developed with the inclusion of the stiffened equation of state for water. The mixture model is considered, where the gas and water inside a computational cell achieve the equilibrium state, with equal pressure, velocity and temperature, within a time step. The splitting method is adopted to calculate the flux of each component at a cell interface individually. The preliminary application of the present newly developed method in different types of shock tube problems, including gas–gas shock tube and gas–water shock tube problems, validates its good performance for gas–water flow.

1. Introduction

The gas–water two-phase flow is a traditional research topic, but it has been still difficult. A typical problem is the underwater high temperature gas flow which involves complex flow physics, such as the formation and expansion of the high temperature gas bubble, the mixing of gas and water, and the phase transition. One of the great difficulties for a computational fluid dynamics (CFD) method is the strongly unsteady interactions of the high temperature gas and the surrounding nearly incompressible water. Existing studies usually solve the gas and the water field separately, with the help of interface capture/tracking technique, such as the level-set, volume of fluid and ghost fluid method. Another way is to directly compute the mixture of gas and water, which is simpler and more robust, especially when the pressure of the gas is not very high [1–5]. Moreover, in some cases a clear interface between gas and water is not interested in, as can be easily found in many industrial fields. However, it is still a challenge to treat the flow with both highly compressible gas and nearly incompressible water.

Based on the Bhatnagar–Gross–Krook (BGK) model of Boltzmann equation, an accurate Navier–Stokes flow solver, the gas-kinetic BGK scheme has been developed in the past decade [6]. Its inherent properties, such as the positivity preserving and the satisfaction of the entropy condition, guarantee the good performance for a wide range of flow physics, including hypersonic flow [7,8] and compressible turbulence [9]. The scheme has been extended to multimaterial gas flows, with individual gas distribution function for each component [10,11], or using a passive scalar to simulate the mass fraction [12,13]. For liquid/gas two-phase flow close to the critical point region, a gas-kinetic scheme has been successfully constructed with the help of the van der Waals equation of state (EOS) [14]. To simulate the Euler equations for one component real gas, a simple extension is to modify the internal degrees of freedom according to the general equation of state [15].

In the present study, a new one-dimensional (1D) gas-kinetic BGK scheme for gas–water two-phase flow is developed based on the mixture model (homogeneous-equilibrium model), along with the stiffened EOS for water. Its performance is then validated with some typical test cases.

* Corresponding author. Tel.: +86 10 62788674; fax: +86 10 62772915.
E-mail addresses: lqb@tsinghua.edu.cn (Q. Li), fs-dem@tsinghua.edu.cn (S. Fu).

0898-1221/$ – see front matter
doi:10.1016/j.camwa.2010.10.016

2. Gas-kinetic BGK scheme for one component flow

As will be mentioned in Section 3, in the present study, the splitting method is adopted to calculate the flux at a cell interface for each component of a multimaterial flow, thus the new scheme can be developed from the direct extension of the method for single component flow. The existing gas-kinetic BGK scheme for one component flow [6] can be briefly introduced in the following.

The one-dimensional BGK equation can be written as

$$\frac{\partial f}{\partial t} + u\frac{\partial f}{\partial x} = \frac{g - f}{\tau}, \tag{1}$$

where f is the gas distribution function and g is the equilibrium state approached by f. Both f and g are functions of space x, time t, particle velocities u, and internal variable ξ. The particle collision time τ is related to the viscosity and heat conduction coefficients. The equilibrium state is a Maxwellian distribution,

$$g = \rho(2\pi RT)^{-\frac{K+1}{2}} \mathrm{e}^{-\frac{(u-U)^2+\xi^2}{2RT}},$$

where ρ is the density, U the macroscopic velocity in the x-direction, R the gas constant, and T the temperature. For a one-dimensional flow, the total number of degrees of freedom K in $\boldsymbol{\xi}$ is equal to $(3-\gamma)/(\gamma-1)$, where the particle motion in the y- and z-directions are also included. The relations between macro conservative variable $\boldsymbol{Q}$ and its flux $\boldsymbol{F}$ with the distribution function f are

$$\boldsymbol{Q} = (\rho, \rho U, \rho E)^T = \int \boldsymbol{\psi} f \mathrm{d}\Xi, \qquad \boldsymbol{F} = \int u f \boldsymbol{\psi} \mathrm{d}\Xi, \tag{2}$$

where $\boldsymbol{\psi}$ is the vector of the moments

$$\boldsymbol{\psi} = (\psi_1, \psi_2, \psi_3)^T = \left(1, u, \frac{1}{2}\left(u^2 + \boldsymbol{\xi}^2\right)\right)^T,$$

and $\mathrm{d}\Xi = \mathrm{d}u\mathrm{d}\xi_1\mathrm{d}\xi_2 \ldots \mathrm{d}\xi_K$ is the volume element in the phase space. Since mass, momentum, and energy are conserved during particle collisions, f and g satisfy the conservation constraint,

$$\int (g - f)\psi_\beta \mathrm{d}\Xi = 0, \quad \beta = 1, 2, 3, \tag{3}$$

at any point in space and time.

From Eqs. (1) and (3), the finite volume formulation of the BGK scheme is formed as

$$\boldsymbol{Q}_i^{n+1} = \boldsymbol{Q}_i^n + \frac{1}{\Delta x_i}\int_{t^n}^{t^n+\Delta t} \boldsymbol{F} \mathrm{d}t \tag{4}$$

where Δx_i is the volume of the ith computational cell. For convenience, the calculation of $\boldsymbol{F}$ is presented through an example at a cell interface $x_{i+1/2} = 0$.

The BGK Eq. (1) has the integral solution for constant collision time τ,

$$f(x, t, u, \boldsymbol{\xi}) = \frac{1}{\tau}\int_0^t g(x', t', u, \boldsymbol{\xi})\mathrm{e}^{-(t-t')/\tau}\mathrm{d}t' + \mathrm{e}^{-t/\tau} f_0(x - ut, u, \boldsymbol{\xi}), \tag{5}$$

where $x' = x - u(t - t')$ is the trajectory of a particle motion and f_0 is the initial gas distribution function at the beginning of each time step ($t = 0$). Here the local constant collision time is calculated based on the local viscosity and pressure, $\tau = \mu/p$.

If f_0 and g are known, the time dependent distribution function f can be easily deduced through the above expression, avoiding the great difficulty to solve the BGK equation directly. In fact, this idea is adopted by the gas-kinetic BGK scheme, with the key to construct f_0 and g around the cell interface $i + 1/2$ according to the Chapman–Enskog expansion,

$$f_0(x, u, \boldsymbol{\xi}) = \left(1 + a^l x - \tau\left(a^l u + A^l\right)\right)(1 - \mathrm{H}[x])g^l + \left(1 + a^r x - \tau\left(a^r u + A^r\right)\right)\mathrm{H}[x]g^r, \tag{6}$$

$$g(x, t, u, \boldsymbol{\xi}) = \left(1 + (1 - \mathrm{H}[x])\overline{a}^l x + \mathrm{H}[x]\overline{a}^r x + \overline{A}t\right)g_0, \tag{7}$$

where g^l, g^r, and g_0 are local Maxwellians, obtained from the initial reconstructed conservative flow variables and their corresponding slopes. Superscripts l and r denote the left and right sides of a cell interface. $\mathrm{H}[x]$ is the Heaviside function of a local coordinate x. The local terms a^l, a^r, $\overline{a}^l$, $\overline{a}^r$, A^l, A^r and $\overline{A}$ are from the Taylor expansion of a Maxwellian and take the form, $a^l = a^l_\beta\psi_\beta$, $\beta = 1$–3, where all coefficients, $a^l_\beta, \ldots, \overline{A}_\beta$, are local constants and evaluated from the spatial and temporal slopes of the reconstructed conservative variables $\boldsymbol{Q}$.

Thus, the distribution function, f, at a cell interface can be obtained through Eq. (5),

$$f(0,t,u,\boldsymbol{\xi}) = (1-C)g_0 + (t+\tau(C-1))\overline{A}g_0 + (tC+\tau(C-1))\left(\overline{a}^l u\mathrm{H}[u] + \overline{a}^r u(1-\mathrm{H}[u])\right)g_0 + C\left(\left(1-(t+\tau)a^l u - \tau A^l\right)\mathrm{H}[u]g^l + \left(1-(t+\tau)a^r u - \tau A^r\right)(1-\mathrm{H}[u])g^r\right), \tag{8}$$

where C is defined as $C = \mathrm{e}^{-t/\tau}$. Then the fluxes across the cell interface can be calculated with Eq. (2) and the conservative variables at the next time step can be calculated via the finite volume formulation (4). Details of the scheme can be found in Refs. [6,13].

3. Gas-kinetic BGK scheme for gas–water flow

For multimaterial gas flows, a simple way to extend the BGK scheme is to include a passive scalar to simulate the mass fraction [12,13]. Another is to adopt individual gas distribution function for each component [10,11], which possesses of the good capability to take into account the interaction between different components, and the flexibility to treat non-perfect gas, such as the stiffened water model [16] considered in the present study. The equation of state of this model is written as

$$p_w = \rho_w R_w T_w - p_c, \tag{9}$$

$$e_w = \frac{R_w T_w}{\gamma_w - 1} + \frac{p_c}{\rho_w} \tag{10}$$

where p_w, T_w, ρ_w and e_w are the pressure, temperature, density and internal energy, respectively. The constant R_w is determined by the specific heat ratio and the specific heat capacity, $R_w = (\gamma_w - 1)/\gamma_w C_{pw}$. The parameters (γ_w, C_{pw}, p_c) are constants based on experimental data. The corresponding sound speed of water for this model can be derived as

$$a_w(T_w) = \sqrt{\gamma_w \frac{p_w + p_c}{\rho_w}}.$$

In the present study, a mixture model is adopted, under the assumption that the gas and water achieve the dynamic and thermal equilibria with equal temperature, pressure and velocity within a computational cell during a time step,

$$p_g = p_w = p, \qquad T_g = T_w = T, \qquad U_g = U_w = U. \tag{11}$$

This is different from gas–gas model where the law of partial pressure works. It should be mentioned that this local equilibrium assumption inside a cell means the relaxation times for the momentum and energy exchanges between gas and water are much less than a computational time step. When the velocity slip or temperature jump between components become important to the flow, non-equilibrium multi-fluid models are more suitable [2,3]. However, although this so called homogeneous-equilibrium model has the limitation in capturing detailed interphasic flow physics, it has been widely used [5] due to its computational efficiency and conservative form. Here the phase change is not considered.

For simplicity, the splitting method is adopted to calculate the flux at a cell interface, thus the subroutines for the scheme for one component can be used directly. The gas and water are described by individual distribution functions,

$$f_g = f_g(x,t,u,\boldsymbol{\xi}), \qquad g_g = \rho_g\left(2\pi R_g T\right)^{-\frac{K_g+1}{2}} \mathrm{e}^{-\frac{(u-U)^2+\boldsymbol{\xi}^2}{2R_g T}}, \tag{12}$$

$$f_w = f_w(x,t,u,\boldsymbol{\xi}), \qquad g_w = \rho_w\left(2\pi R_w T\right)^{-\frac{K_w+1}{2}} \mathrm{e}^{-\frac{(u-U)^2+\boldsymbol{\xi}^2}{2R_w T}}. \tag{13}$$

With the help of gas volume fraction, denoted by α, the macro conservative variables can be calculated through the integration of the distributions

$$\boldsymbol{Q} = \left(\alpha\rho_g, (1-\alpha)\rho_w, \rho U, \rho E\right)^T = \alpha\int \boldsymbol{\psi}_g f_g \mathrm{d}\Xi + (1-\alpha)\int \boldsymbol{\psi}_w f_w \mathrm{d}\Xi + [0,0,0,(1-\alpha)p_c]^T, \tag{14}$$

where the density and total energy are

$$\rho = \alpha\rho_g + (1-\alpha)\rho_w, \tag{15}$$

$$\rho E = \alpha\frac{\rho_g R_g T}{\gamma_g - 1} + (1-\alpha)\left[\frac{\rho_w R_w T}{\gamma_w - 1} + p_c\right] + \frac{1}{2}\rho U^2, \tag{16}$$

and two moment vectors are required,

$$\boldsymbol{\psi}_g = \left(1, 0, u, \frac{1}{2}\left(u^2+\boldsymbol{\xi}^2\right)\right)^T, \qquad \boldsymbol{\psi}_w = \left(0, 1, u, \frac{1}{2}\left(u^2+\boldsymbol{\xi}^2\right)\right)^T.$$

Then the flux at a cell interface is obtained by

$$\boldsymbol{F} = \alpha \int u\boldsymbol{\psi}_g f_g \mathrm{d}\Xi + (1-\alpha)\int u\boldsymbol{\psi}_w f_w \mathrm{d}\Xi + [0, 0, \delta p, U(\delta p + (1-\alpha)p_c)]^T, \tag{17}$$

where the third component of the last term on the right side comes from the mixing of gas and water, which resulting in the modification of the pressure from $[\alpha p_{gf} + (1-\alpha)p_{wf}]$ to the equilibrium value p. Here the subscript 'f' indicates the calculation from the distribution function directly, neglecting the effect of p_c in the stiffened EOS. Thus the pressure correction is

$$\begin{aligned}\delta p &= p - \left[\alpha p_{gf} + (1-\alpha)p_{wf}\right] \\ &= p - \left[\alpha\rho_g R_g + (1-\alpha)\rho_w R_w\right] T,\end{aligned} \tag{18}$$

and the equilibrium temperature T is computed from the total energy component of $\boldsymbol{Q}$ (see Eq. (14)),

$$T = \frac{\rho E - \frac{1}{2}\rho U^2 - (1-\alpha)p_c}{\frac{\alpha\rho_g R_g}{\gamma_g - 1} + \frac{(1-\alpha)\rho_w R_w}{\gamma_w - 1}}. \tag{19}$$

The fourth component of the last term in Eq. (17) is the contribution by both the pressure correction due to mixing and the constant pressure p_c in the total energy itself. However, for the perfect gas mixture, $p_c = 0$, the last term in Eq. (17) automatically goes to zero, then the above correction is not necessary.

Till now the only unknown variable is the volume fraction α. It can be calculated by the first two components of $\boldsymbol{Q}$, $Q_1 = \alpha\rho_g$, $Q_2 = (1-\alpha)\rho_w$, combined with the equilibrium condition for pressure, $p_g = p_w$, which leads to a quadratic equation

$$\frac{Q_1 R_g T}{\alpha} = \frac{Q_2 R_w T}{1-\alpha} - p_c, \tag{20}$$

and thus the volume fraction can be determined by the positive root of the above equation. To increase the temporal accuracy, quantities at the cell interface computed directly from the distribution function (Eqs. (8) and (14)), such as Q_1, Q_2 in the above equation are chosen as the time-average within a time step.

It should be noted that the above-presented method is a viscous flow solver and the collision time can be calculated by the viscosity of the gas/water mixture. For inviscid flow, the collision time is determined by

$$\tau = C_1\Delta t + C_2\Delta t\frac{|p^l - p^r|}{p^l + p^r}, \tag{21}$$

where p^l, p^r are the reconstructed pressure at two sides of a cell interface, and the values of constants C_1, C_2 can be set between 0 and 1. Another point is that if we set $p_c = 0$, the previous scheme for perfect gas mixture can be recovered automatically.

4. Numerical examples

The present gas-kinetic BGK scheme is then validated by four different shock tube problems, including the gas–gas flow and several water–air flows with different initial pressure jump and void fraction. Unless otherwise stated, the computational domain is [0, 10] divided by N uniform cells. The initial discontinuity is located at $x = 5$. In all numerical examples reported here, the CFL number is set to 0.3 and all variables are presented in the SI units. These cases are inviscid and the collision time is calculated by Eq. (21).

4.1. Gas–gas shock tube problem

The first test case is a shock tube problem for two gases [10] with constants $(\gamma_1, R_1, \gamma_2, R_2) = (1.4, 1, 1.2, 1)$ and $p_c = 0$. The flow field is initialized with

$$(\alpha, U, p, T)_L = (\epsilon, 0, 1, 1), \qquad (\alpha, U, p, T)_R = (1-\epsilon, 0, 0.1, 0.8).$$

Here $\epsilon = 10^{-7}$ is adopted. Figs. 1–5 show the simulated flow field at time $t = 2.5$. One can observe that the present results agree very well with those computed by the gas-kinetic BGK scheme for multicomponent gas flow [10]. The shock wave, the rarefaction wave, and the contact line are well captured by the present method. The interface of two gases is smooth, across about ten cells, which comes from the inherent characteristics of the mixture model. The mixing of different gases can smear the sharp discontinuity. However, here it is a numerical mixing as we just consider the inviscid case. With a proper viscosity model, this mixing process can be simulated by the present scheme.

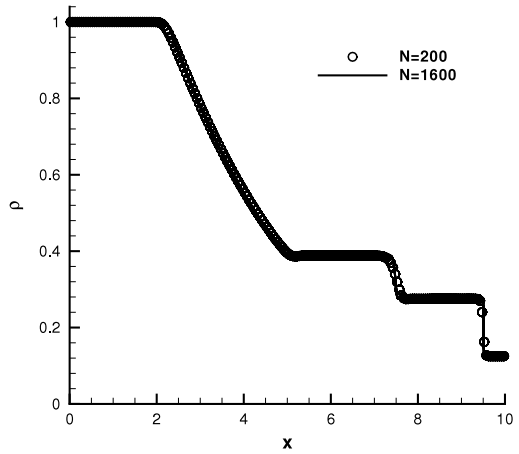

Fig. 1. Total density distribution of gas–gas shock tube problem.

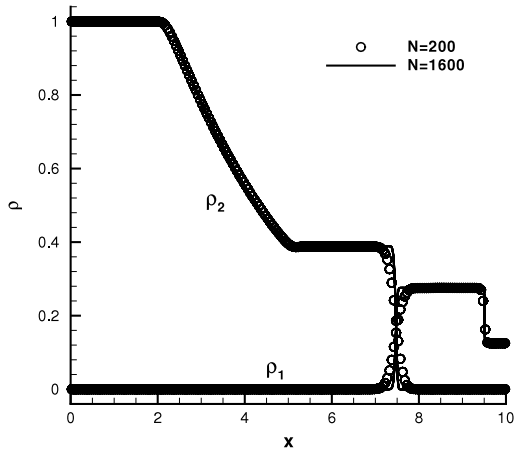

Fig. 2. Density profiles of gas–gas shock tube problem.

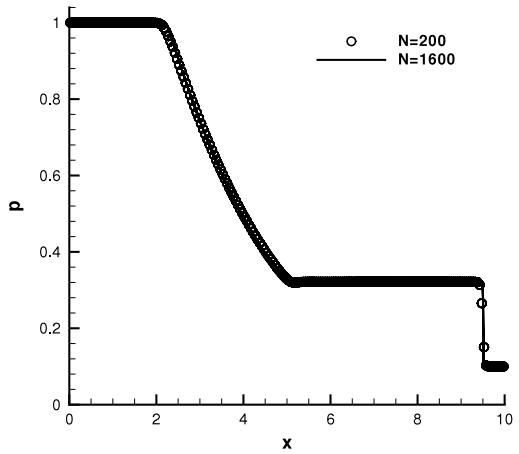

Fig. 3. Pressure distribution of gas–gas shock tube problem.

4.2. Air-to-water shock tube problem

The second test case is an air–water shock tube problem with large pressure ratio of 10^4 [3]. The constants for air is $(\gamma_g, R_g, p_c) = (1.4, 288, 0)$, and $(\gamma_w, C_{pw}, p_c) = (1.9276, 8076.6, 1.1378 \times 10^9)$ for water. The initial conditions are set as

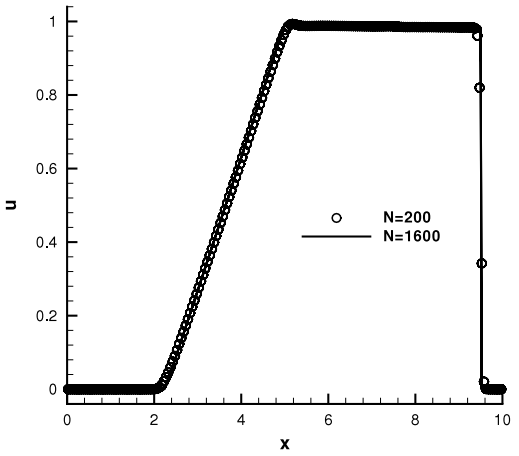

Fig. 4. Velocity distribution of gas–gas shock tube problem.

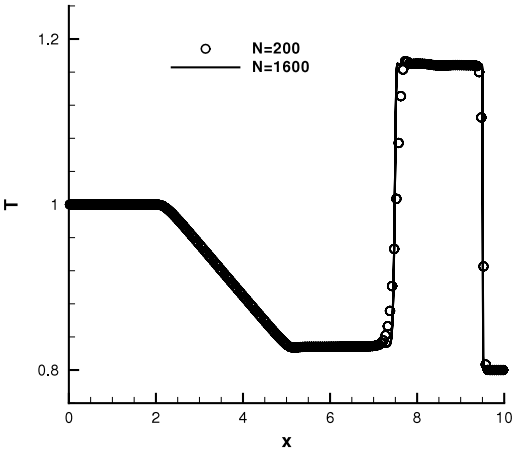

Fig. 5. Temperature distribution of gas–gas shock tube problem.

follows:

$$(\alpha, U, p, T)_L = \left(1-\epsilon, 0, 10^9, 308.15\right), \qquad (\alpha, U, p, T)_R = \left(\epsilon, 0, 10^5, 308.15\right),$$

where $\epsilon = 10^{-5}$ is used.

Figs. 6–10 present the predicted results at time $t = 2.35 \times 10^{-3}$, from which the very strong shock transmitting into the water, the rarefaction wave travelling back into the air, and the fluid interface can be observed with good resolution. The present results agree well with Chang and Liou's study [3] using a stratified flow model, except for the small stick in the velocity near the interface. This is from the present mixture model, with the equal temperature and velocity assumption in a cell, which means the redistribution of inner energy, resulting in the variation of kinetic energy under the constraint of the conservation of total energy. It should be mentioned that in gas–water flow the speed of a travelling wave predicted by different mixture models may be quite different. However, in this case, the shock and rarefaction wave travel in nearly pure gas or water, so their speeds predicted by the present method with homogeneous-equilibrium mixture model agree with those from a stratified flow model.

4.3. Shock tube problem in air–water mixture

The third case is a shock tube problem in air–water mixture with uniform initial mass fraction. The computational domain is [0, 1] and the initial discontinuity is located at $x = 0.5$. The initial conditions are set as follows:

$$(\alpha, U, p, T)_L = \left(0.8013, 0, 2 \times 10^7, 300\right),$$

$$(\alpha, U, p, T)_R = \left(0.8412, 0, 1.5 \times 10^7, 300\right).$$

To compare with the existing results predicted by Ihm and Kim with HEM model [5], we chose the constants for water is $(\gamma_w, C_{pw}, p_c) = (2.8, 4186, 7.367 \times 10^8)$, which can ensure the accuracy of sound speed and specific heat. However, the compressibility based on these constants shows a minor difference with that in the reference.

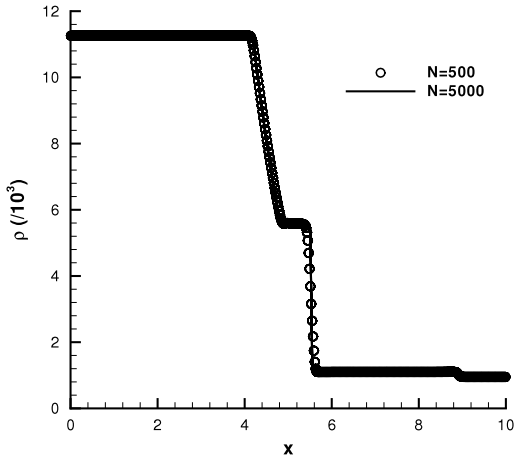

Fig. 6. Total density distribution of air–water shock tube problem.

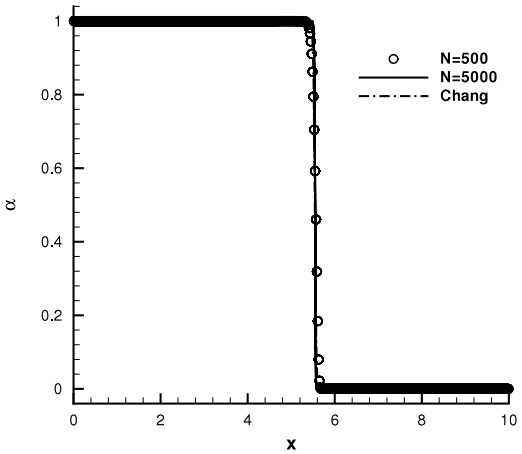

Fig. 7. Air void fraction profiles of air–water shock tube problem.

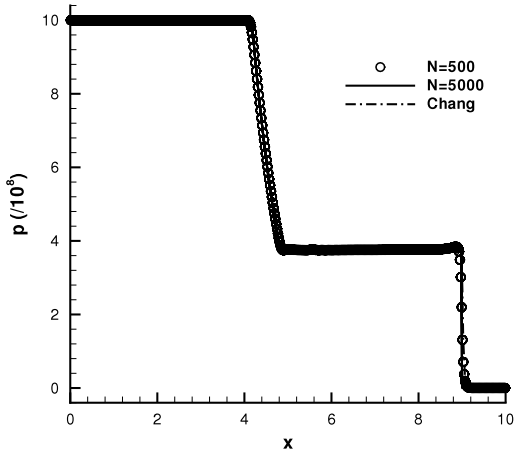

Fig. 8. Pressure profiles of air–water shock tube problem.

Figs. 11–15 show the computed results at time $t = 1 \times 10^{-3}$, which agree well with Ihm and Kim's prediction. The deviation of air void fraction may come from the different EOS for water.

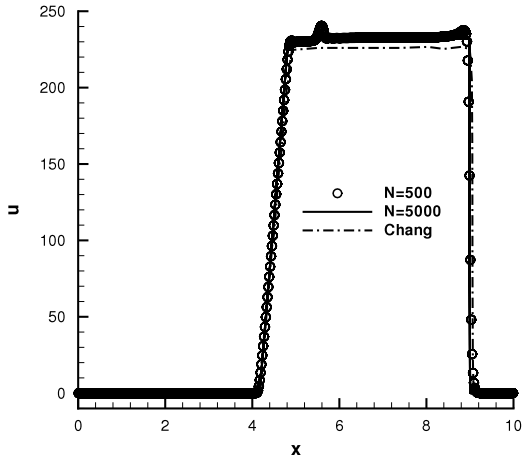

Fig. 9. Velocity profiles of air–water shock tube problem.

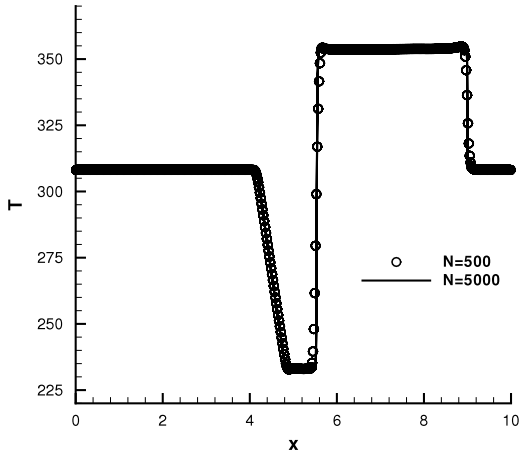

Fig. 10. Temperature distribution of air–water shock tube problem.

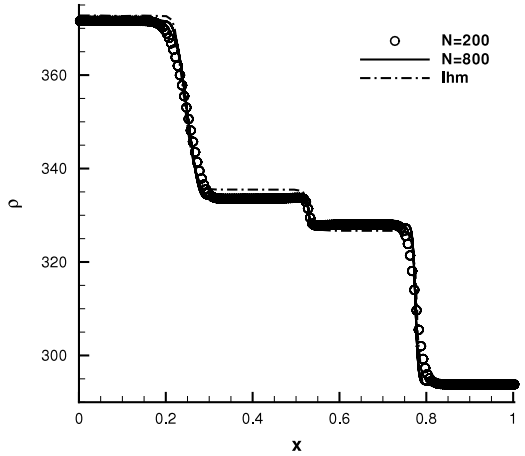

Fig. 11. Total density distribution of shock tube problem in air–water mixture.

4.4. Water–air shock tube problem

The last test case is also a two-fluid shock tube problem [2,4,17]. The constants are chosen as $(\gamma_g, R_g, p_c) = (1.4, 288, 0)$ for air and $(\gamma_w, C_{pw}, p_c) = (2.8, 4186, 8.5 \times 10^8)$ for water. The initial flow field is given by

$$(\alpha, U, p, T)_L = \left(0.25, 0, 2 \times 10^7, 308.15\right), \qquad (\alpha, U, p, T)_R = \left(0.1, 0, 10^7, 308.15\right).$$

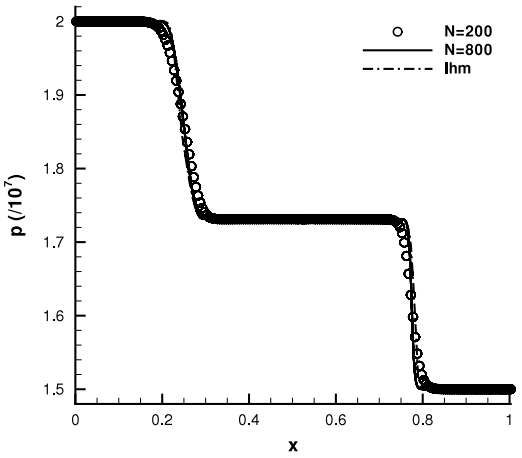

Fig. 12. Pressure profiles of shock tube problem in air–water mixture.

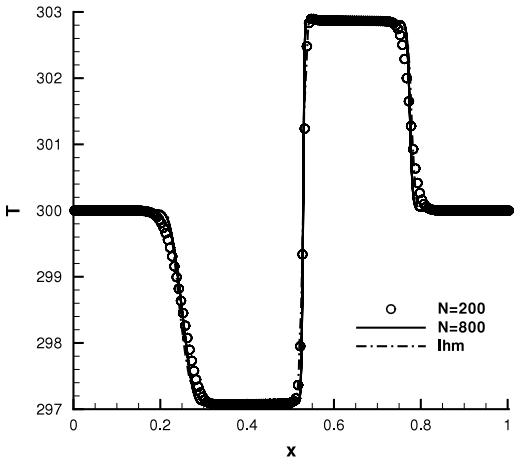

Fig. 13. Temperature distribution of shock tube problem in air–water mixture.

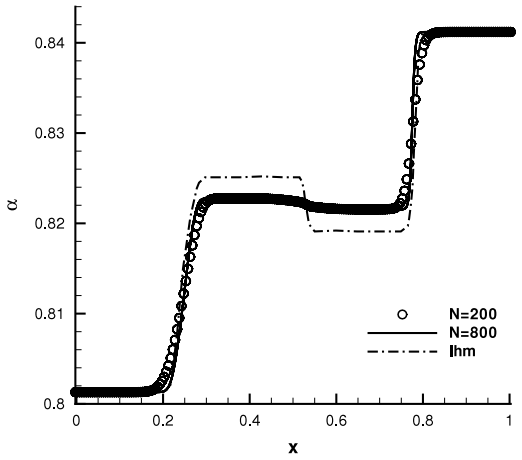

Fig. 14. Gas void fraction profiles of shock tube problem in air–water mixture.

The simulated results at time $t = 6 \times 10^{-3}$ are shown in Figs. 16–20. Again the expansion wave, the shock wave and the contact discontinuity are well captured, although with the present mixture model we can only obtain the averaged temperature and velocity. However, there is a little oscillation of temperature at the interface, although the amplitude is

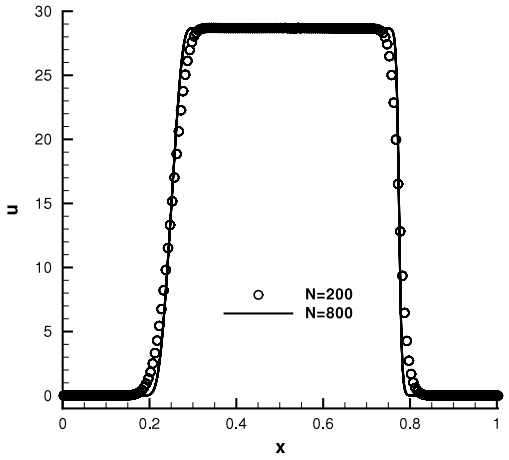

Fig. 15. Velocity profiles of shock tube problem in air–water mixture.

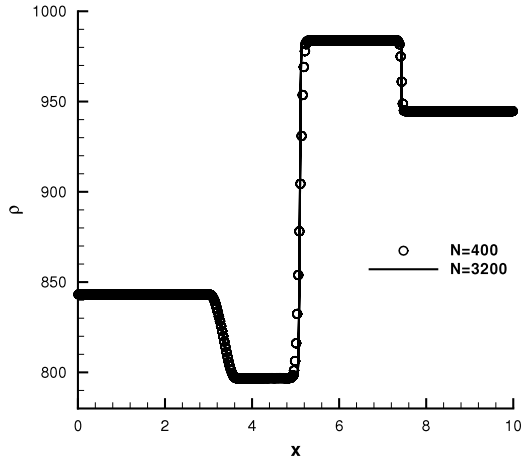

Fig. 16. Total density distribution of water–air shock tube problem with initial gas void fraction $(\alpha_L, \alpha_R) = (0.25, 0.1)$.

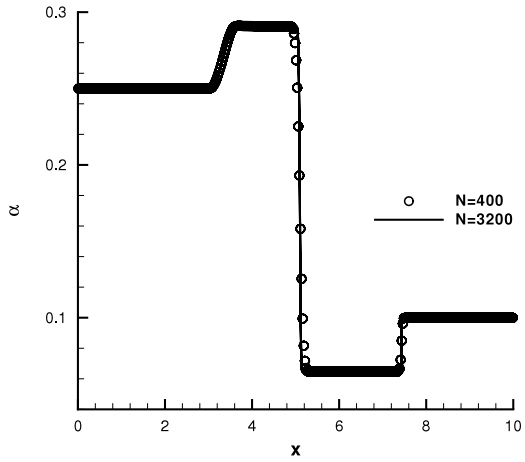

Fig. 17. Void fraction distribution of water–air shock tube problem with initial gas void fraction $(\alpha_L, \alpha_R) = (0.25, 0.1)$.

less than 0.5 K. This may be caused by the numerical dissipation, as it disappears when increasing the computational cell number.

To further validate the present method, we change the initial void fraction on the right side to $\alpha_R = 0.75$, which is more challenge as shock wave will transmit from water into air. The results at time $t = 6 \times 10^{-3}$ are shown in Figs. 21–25.

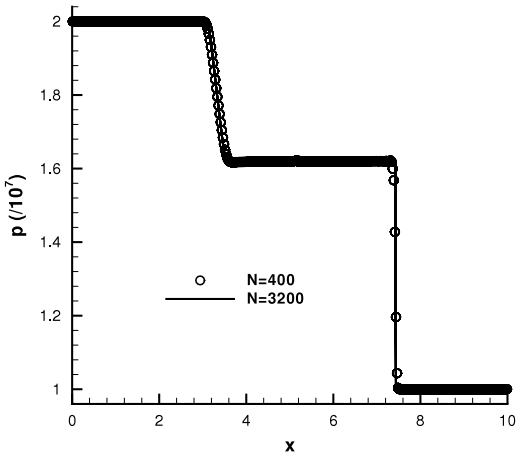

Fig. 18. Pressure distribution of water–air shock tube problem with initial gas void fraction $(\alpha_L, \alpha_R) = (0.25, 0.1)$.

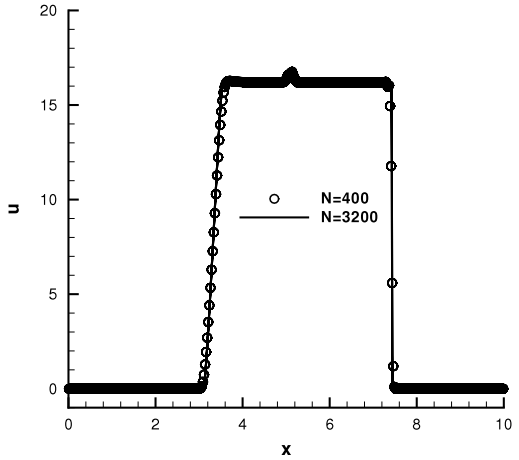

Fig. 19. Velocity distribution of water–air shock tube problem with initial gas void fraction $(\alpha_L, \alpha_R) = (0.25, 0.1)$.

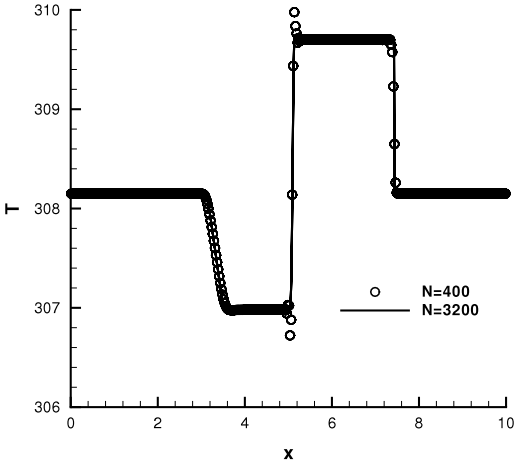

Fig. 20. Temperature distribution of water–air shock tube problem with initial gas void fraction $(\alpha_L, \alpha_R) = (0.25, 0.1)$.

Once again the expansion wave, the shock wave and the contact discontinuity are well captured, and the temperature at the interface shows a little oscillation on a coarse mesh. We have also tried some much more challenge cases, such as the shock wave transmits from nearly pure water to nearly pure gas, and found that the robustness of the present scheme may become less than satisfactory. However, under these extreme conditions, it is questionable to adopt the homogeneous-equilibrium

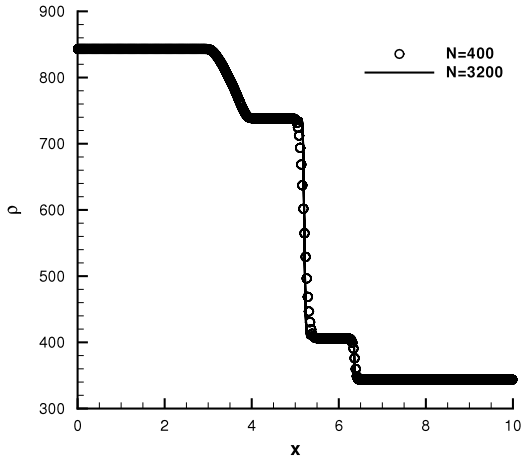

Fig. 21. Total density distribution of water–air shock tube problem with initial gas void fraction $(\alpha_L, \alpha_R) = (0.25, 0.75)$.

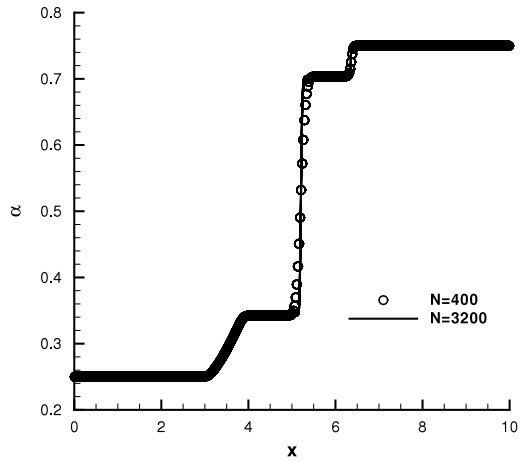

Fig. 22. Void fraction distribution of water–air shock tube problem with initial gas void fraction $(\alpha_L, \alpha_R) = (0.25, 0.75)$.

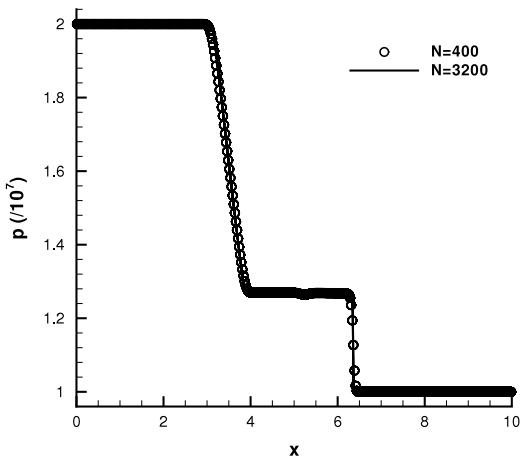

Fig. 23. Pressure distribution of water–air shock tube problem with initial gas void fraction $(\alpha_L, \alpha_R) = (0.25, 0.75)$.

mixture model. Thus a more reasonable mixture model and a more suitable method to determine the void fraction at a cell interface are required in the further study.

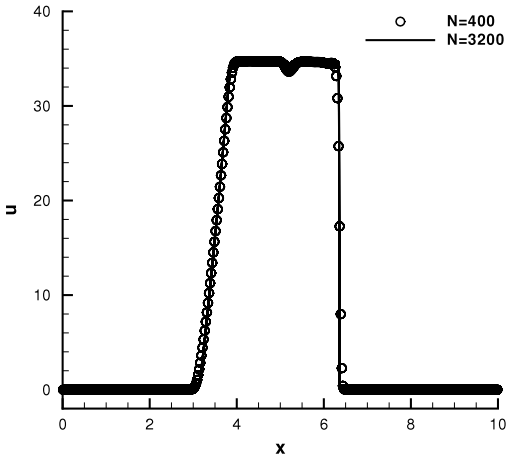

Fig. 24. Velocity distribution of water–air shock tube problem with initial gas void fraction $(\alpha_L, \alpha_R) = (0.25, 0.75)$.

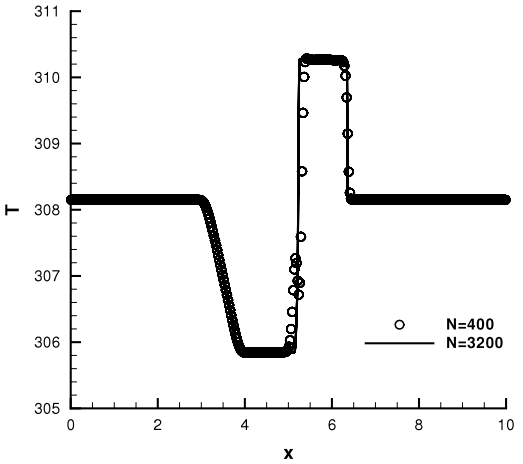

Fig. 25. Temperature distribution of water–air shock tube problem with initial gas void fraction $(\alpha_L, \alpha_R) = (0.25, 0.75)$.

5. Conclusion and discussion

A gas-kinetic BGK scheme for gas–water flow is constructed with the splitting method to calculate the flux of different fluid at a cell interface individually. The stiffened equation of state for water is adopted and the mixture model is considered under the assumption of equal pressure, temperature and velocity of different fluids inside a computational cell. The application of the present newly developed method in different types of shock tube problems, including gas–gas flow and gas–water cases, validates its good performance for gas–water flow. Additionally, it is simple for the present method to be developed from the one component version, and it is also convenient to be extended to two-dimensional flow. However, the effect of this splitting treatment, as well as the capability in viscous flow, still requires further investigation. A more suitable mixture model for the present method to take into account the non-equilibrium effect inside a cell, such as the velocity slip and temperature jump between each phase, is also worthy of study.

Acknowledgements

This work is supported by National Natural Science Foundation of China (Project No. 10872112) and Science and Technology Innovation foundation of CASC.

References

[1] R. Abgrall, R. Saurel, Discrete equations for physical and numerical compressible multiphase mixtures, J. Comput. Phys. 186 (2003) 361–396.
[2] H. Paillère, C. Corre, J.R.G. Cascales, On the extension of the AUSM+ scheme to compressible two-fluid models, Comput. & Fluids 32 (2003) 891–916.
[3] C.-H. Chang, M.-S. Liou, A robust and accurate approach to computing compressible multiphase flow: Stratified flow model and AUSM+-up scheme, J. Comput. Phys. 225 (2007) 840–873.

[4] Y.-Y. Niu, Y.C. Lin, C.-H. Chang, A further work on multi-phase two-fluid approach for compressible multi-phase flows, Internat. J. Numer. Methods Fluids 58 (2008) 879–896.
[5] S.-W. Ihm, C. Kim, Computations of homogeneous-equibrium two-phase flow with accurate and efficient shock-stable schemes, AIAA J. 46 (12) (2008) 3012–3037.
[6] K. Xu, A gas-kinetic BGK scheme for the Navier–Stokes equations, and its connection with artificial dissipation and Godunov method, J. Comput. Phys. 171 (2001) 289–335.
[7] K. Xu, M. Mao, L. Tang, A multidimensional gas-kinetic BGK scheme for hypersonic viscous flow, J. Comput. Phys. 203 (2005) 405–421.
[8] Q.B. Li, S. Fu, K. Xu, Application of gas-kinetic scheme with kinetic boundary conditions in hypersonic flow, AIAA J. 43 (10) (2005) 2170–2176.
[9] Q.B. Li, S. Fu, Numerical simulation of high-speed planar mixing layer, Comput. & Fluids 32 (2003) 1357–1377.
[10] K. Xu, BGK-based scheme for multicomponent flow calculations, J. Comput. Phys. 134 (1997) 122–133.
[11] Y.S. Lian, K. Xu, A gas-kinetic scheme for multimaterial flows and its application in chemical reactions, J. Comput. Phys. 163 (2000) 349–375.
[12] Y.S. Lian, K. Xu, A gas-kinetic scheme for reactive flows, Comput. & Fluids 29 (7) (2000) 725–748.
[13] Q.B. Li, S. Fu, K. Xu, A compressible Navier–Stokes flow solver with scalar transport, J. Comput. Phys. 204 (2005) 692–714.
[14] K. Xu, A kinetic method for hyperbolic-elliptic equations and its application in two-phase flow, J. Comput. Phys. 166 (2001) 383–399.
[15] H.Z. Tang, Gas-kinetic scheme for compressible flow of real gases, Comput. Math. Appl. 41 (2001) 723–734.
[16] F. Harlow, A. Amsden, Fluid dynamics. Technical report, Los Alamos National Laboratory, 1971. LA-4700.
[17] I. Toumi, An upwind numerical method for two-fluid two-phase flow models, Nucl. Sci. Eng. 123 (1996) 147–168.